Cooling molecules in optical cavities

Weiping Lu and Yongkai Zhao
Physics, School of Engineering and Physical Sciences, Heriot-Watt University, Edinburgh EH14 4AS, United Kingdom

P. F. Barker
Department of Physics and Astronomy, University College London, London WC1E 6BT, United Kingdom
(Received 20 March 2007; published 25 July 2007)

We have studied theoretically and numerically the cooling of CN molecules in a high-finesse optical cavity and show that these molecules can be cooled from 100 mK temperatures to submillikelvin temperatures in less than 1 ms. We establish that the cooling time does not change significantly with molecular numbers and initial temperatures over a wide range. We have further studied the scaling of the system for extending the current results for hundreds of molecules to a very large molecular ensemble. The results indicate that a gas of 10^9 molecules can be cooled in the cavity by use of a far-off-resonant and high-intensity pump source.

DOI: 10.1103/PhysRevA.76.013417 PACS number(s): 33.80.Ps, 32.80.Lg, 42.50.Fx, 42.50.Vk

Over the past few decades, physicists have learned to cool atoms and molecules to microkelvin and nanokelvin temperatures. Cold atoms are now the basis of many new areas of fundamental physics and technology, and are central to the production of Bose-Einstein condensates, atomic clocks, and matter-wave interferometers. To produce cold dense atomic samples, laser-cooling schemes use many consecutive absorption-emission cycles in a closed multilevel system to extract kinetic energy from the atoms [1]. There is now significant interest within the physics and chemistry communities to create ultracold molecules for precision molecular measurements, ultracold chemistry, and for exploring strongly correlated dipolar molecular gases. Molecules, however, cannot be laser cooled because of their complex energy structure which precludes the closed-cycling transition necessary for laser cooling. While some ultracold molecules can be created by association of laser-cooled atoms, several groups around the world have been developing alternative, more general methods to produce cold molecular species. Among these methods are buffer gas cooling, which is capable of producing and trapping cold paramagnetic molecules at temperatures in the 100 mK range [2,3]. Other techniques such as Stark deceleration can also create molecules down to the 10 mK temperature range [4,5]. However, much of the interesting physics and chemistry is predicted to occur at lower temperatures in the microkelvin range, and thus new dissipative cooling schemes are required.

It has been observed that the coupled atom-field dynamics in an optical cavity can lead to a friction force that damps atomic motion [6,7]. This scheme is commonly called cavity cooling. Since dissipation takes place via cavity loss rather than by spontaneous emission, cavity cooling avoids or reduces several problems of the laser-cooling scheme, such as photon reabsorption and recoil heating. Moreover, as there is no requirement in cavity cooling for a closed multilevel system, it is an attractive approach for creating ultracold molecules. In cavity cooling, all atoms within the cavity are coupled to the same field modes. When the cavity is pumped along the cavity axis, atomic cross talk is found to significantly increase the cooling time, since the atoms are randomly distributed and individual effects of the atom-field interaction can cancel each other. For this configuration a linear increase of the cooling time with atom number has been predicted [8], which makes this scheme impractical for cooling a large number of atoms. In a recent study, however, it was shown that, when the intracavity field is generated through atom-mediated scattering of a pump source from the direction transverse to the cavity axis, an additional force on the atoms arising from the pump–intracavity-field interference can lead to spatial self-organization and localization of the atom [9]. The scaling laws in this scheme favor cooling of a large atomic sample and an experimental demonstration of cooling 10^6 cesium atoms to a few microkelvin has been observed using this scheme [10].

In this paper we explore how this transverse cavity cooling scheme can be extended to the diatomic molecule CN. The present work provides several important findings beyond the scope of previous investigations on cooling atoms in optical cavities [9,11]. We find that molecule-field interaction generally involves multiple molecular energy levels because of their complex energy structure. However, due to the off-resonant nature of the interaction, population transitions can be neglected and the upper levels are consequently unpopulated. This allows us to simplify the model description. We show that a two two-level model is adequate to describe the center-of-mass dynamics of CN molecules in optical cavities. In general, the involvement of multiple levels enhances the molecule-field coupling strength, which is favorable for cavity cooling, particularly for molecules that usually have a weaker coupling strength compared to atoms. Moreover, previous studies have focused primarily on the dynamics and self-organization in the cavities of ultracold atoms that have a temperature close to the cavity cooling limit in microkelvin region. The present work extends the scope of the investigation to cooling of molecules as a consequence of self-organization in the cavities. As molecules at temperatures of a few hundred millikelvins can now be produced, we are particularly interested in cooling these molecular gases to temperatures in the microkelvin region. As an example, we study cooling of a CN molecular gas in a millimeter-long optical cavity and show a reduction of temperature by two orders of magnitude to below 1 mK. We have also studied the effects of untrapped molecules in the cavities on the cooling temperature and cooling time. Untrapped molecules oc-

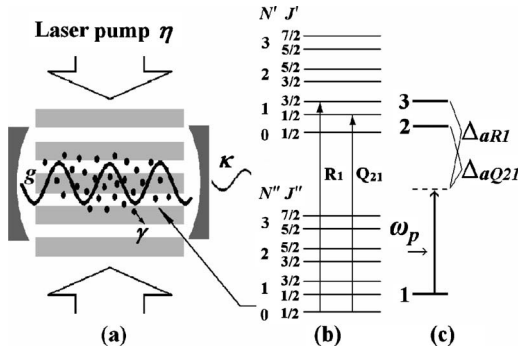

FIG. 1. (a) Schematic of cavity cooling. (b) $(B\text{-}X)$, (0,0) transitions of a CN molecule. (c) The three-levels of the CN molecules which can be simplified as two two-level interactions.

cur when the initial temperature of the molecular gas is much higher than the cavity cooling temperature limit. We find that, after taking into account the loss of untrapped molecules from the cavities, the cooling time of the trapped molecules remains almost the same irrespective of the initial number of molecules and their initial temperature over a wide range. This finding is also true for atoms. We have further investigated stable defect molecules [11] in cavities, and particularly their effects on cavity cooling. We find that molecular self-organization and collective cooling occur only when the molecular number is below a threshold, which is determined by the cavity lifetime and the molecule-field coupling strength. From this finding and also the scaling laws of the system, we show that cavity cooling of a very large molecular sample can be made possible by use of a far-off-resonant, high-intensity pump source. Since far-off-resonant interactions do not rely on specific internal energy levels of particles, cavity cooling operating in this regime can in principle be realized for any polarizable species.

We investigate the center-of-mass motion of N molecules in an optical cavity pumped by a laser source from the direction that is transverse to the cavity axis, as shown in Fig. 1(a). For simplicity, we restrain the model to one dimension in the cavity axis direction. We consider CN molecules in this study because the pump source that is required for the transition is in the uv region for which cavity optics are readily available, and stationary cold molecules could be created using optical Stark deceleration [12]. For this gas in the 100 mK range only the lowest rovibrational energy level is populated. We consider a pump laser source at around 387.6 nm, for which there are only two allowed transition lines as shown in Fig. 1(b). These are the R_1 line, $B\,^2\Sigma^+(v'=0,N'=1,J'=3/2)\leftrightarrow X\,^2\Sigma^+(v''=0,N''=0,J''=1/2)$, and the Q_{21} line, $B\,^2\Sigma^+(v'=0,N'=1,J'=1/2)\leftrightarrow X\,^2\Sigma^+(v''=0,N''=0,J''=1/2)$. The frequency separation of the two is around 5 GHz. A three-level model is therefore sufficient to describe the system, as depicted in Fig. 1(c). Levels $|1\rangle$ and $|3\rangle$ correspond to the R_1 line and levels $|1\rangle$ and $|2\rangle$ to the Q_{21} line. To reduce diffusive heating, we consider a large pump frequency detuning of 15 GHz from the Q_{21} line and 20 GHz from the R_1 line, for which populations in levels $|2\rangle$ and $|3\rangle$ can be neglected. The three-level system can thus be simplified as two two-level interactions. The equations of motion are given by generalizing the two-level model [9,11]

$$\dot{\alpha} = (i\Delta_c - \kappa)\alpha - (\Gamma_0 + iU_0)\sum_j \cos^2(kx_j)\alpha - \eta_{eff}\sum_j \cos(kx_j) + \xi_\alpha, \tag{1a}$$

$$\dot{p}_j = \hbar k U_0\left(|\alpha|^2 - \frac{1}{2}\right)\sin(2kx_j) + i\hbar k(\eta_{eff}^*\alpha - \eta_{eff}\alpha^*)\sin(kx_j) + \xi_{pj}, \tag{1b}$$

$$\dot{x}_j = p_j/m \tag{1c}$$

where $|\alpha|^2$ is the intracavity photon number, p_j the molecular momentum, x_j the position $(j=1,\ldots,N)$, $\Delta_c=\omega-\omega_c$ the pump-cavity detuning, and m the mass of the molecule. The parameters

$$U_0 \equiv U_{R1} + U_{Q21} = \frac{\Delta_{aR1}g_{R1}^2}{\gamma^2+\Delta_{aR1}^2} + \frac{\Delta_{aQ21}g_{Q21}^2}{\gamma^2+\Delta_{aQ21}^2},$$

$$\Gamma_0 \equiv \Gamma_{R1} + \Gamma_{Q21} = \frac{\gamma g_{R1}^2}{\gamma^2+\Delta_{aR1}^2} + \frac{\gamma g_{Q21}^2}{\gamma^2+\Delta_{aQ21}^2} \tag{2}$$

describe the dispersion and absorption of the molecules when both the transition lines are taken into account, where γ is the spontaneous emission linewidth, g_{R1} and g_{Q21} are the coupling strengths of the two lines, and $\Delta_{aR1}=\omega-\omega_{aR1}$ and $\Delta_{aQ21}=\omega-\omega_{aQ21}$ are the pump-molecule detuning for the two lines. The photon number scattered into the cavity by the pump η is $|\eta_{eff}|^2$, where

$$\eta_{eff} = \frac{\eta g_{R1}(\gamma+i\Delta_{aR1})}{\Delta_{aR1}^2+\gamma^2} + \frac{\eta g_{Q21}(\gamma+i\Delta_{aQ21})}{\Delta_{aQ21}^2+\gamma^2}, \tag{3}$$

which also has two terms. The noise terms in Eq. (1) are of a Langevin-type that obeys the following relations:

$$\langle \xi_\alpha^*\xi_\alpha\rangle = \kappa + \Gamma_0\sum_{j=1}^{N}\cos^2(kx_j), \tag{4a}$$

$$\langle \xi_{pj}\xi_\alpha\rangle = -i\hbar k\Gamma_0\alpha\sin(kx_j)\cos(kx_j), \tag{4b}$$

$$\langle \xi_{pj}\xi_{pj}\rangle = 2\hbar^2\Gamma_0 k^2\overline{u^2}|\cos(kx_j)\alpha + \eta/g|^2 + 2\hbar^2k^2\Gamma_0|\alpha|^2\sin^2(kx_j), \tag{4c}$$

where $g=\sqrt{g_{R1}^2+g_{Q21}^2}$. Equation (4) defines, through the second-order correlations, the random fluctuations of the intracavity field, the cross talk between the field and momentum, and the momentum recoil, respectively. In simulations they can be decomposed into uncorrelated and correlated terms $\xi_\alpha=\xi_\alpha^{(0)}+\xi_\alpha^{(1)}$ and $\xi_{pm}=\xi_{pm}^{(0)}+\xi_{pm}^{(1)}$. The correlated terms are given as

$$\xi_{pj}^{(1)} = -\hbar k\sqrt{2\Gamma_0}\sin(kx)|\alpha|\xi_3^{(j)},$$

$$\xi_\alpha^{(1)} = i\frac{\alpha}{|\alpha|}\sqrt{\Gamma_0/2}\sum_{j=1}^{N}\cos(kx_j)\zeta_3^{(j)},$$

and the uncorrelated terms are

$$\xi_\alpha^{(0)} = \left(-\frac{\sqrt{\Gamma_0}}{2}\sum_{j=1}^{N}\cos(kx_i)\zeta_1^{(j)} + \sqrt{\kappa/2}\zeta_r\right) + i\left(\frac{\sqrt{\Gamma_0}}{2}\sum_{j=1}^{N}\cos(kx_i)\zeta_2^{(j)} + \sqrt{\kappa/2}\zeta_i\right),$$

$$\xi_{pj}^{(0)} = \hbar k\sqrt{\overline{u^2}}\sqrt{2\Gamma_0}\left[\left(\alpha_r\cos(kx_j) + \frac{\eta}{g}\right)\zeta_{pj}^1 + \alpha_i\cos(kx_j)\zeta_{pj}^2\right],$$

where $\zeta_1^{(j)}$, $\zeta_2^{(j)}$, $\zeta_3^{(j)}$, ζ_{pj}^1, ζ_{pj}^2, ζ_r, and ζ_i $(j=1,\ldots,N)$ are all independent random numbers with mean 0 and variance 1. The parameter $k\sqrt{\overline{u^2}}$ is the main projection of the momentum recoil along the cavity axis due to the spontaneous emission. In this study, the cavity is set to have the length of $l=1.5$ mm, the finesse of $F=3.1\times10^4$, a mode volume of $V_{eff}=2.6\times10^{-5}$ mm^3, and a cavity linewidth of $\kappa=20$ MHz. The cavity detuning is set to be $\Delta_c=-\kappa+N_{tr}U_0$, where the strong effect of particle position-induced-field variations in the cavity is seen [11]. The spontaneous emission linewidth $\gamma=15.4$ MHz. The pump frequency is detuned to be $\Delta_{aQ21}=-15$ GHz and $\Delta_{aR1}=-20$ GHz, which are much larger than γ. Using the well-documented parameters for $(B\text{-}X)$ (0,0) transitions of the CN molecule [13], we obtain the coupling strengths $g_{R1}=14.1$ MHz, $g_{Q21}=10.0$ MHz and the total coupling strength that combines the two lines $g=\sqrt{{g_{R1}}^2+{g_{Q21}}^2}=17.3$ MHz. In numerical simulations, Eqs. (1)–(3) are normalized to be dimensionless. The momentum p_j is normalized by $1/\hbar k$, the space x by k, and the time t by κ. The parameters g, γ, Δ_c, Δ_a, η_{eff}, and the recoil frequency $\omega_{rec}=\hbar k^2/(2m)$ are normalized by $1/\kappa$. The parameter sets used in the simulations ensure that the molecular population in the upper levels is negligible.

We first study the dynamics of the CN gas in a cavity that has an initial temperature of 100 mK, which is significantly higher than the cavity cooling temperature limit of $\hbar\kappa=150$ μK for our system [6]. Figure 2 shows the evolution of temperature, intracavity photon number, and spatial spreading parameter for 200 CN molecules that are initially placed uniformly in the central region of the cavity. The spreading parameter $k^2\overline{x^2}$ measures the averaged distance of molecules from their nearest antinodes of the intracavity field. When a pump intensity of 54 kW/cm^2 $(\eta=300\kappa)$ is applied to the cavity, the intracavity field rapidly builds up through molecule-mediated scattering. Accompanying this process is the dissipation of the kinetic energy of the molecules owing to the cavity cooling mechanism. This results in molecules becoming trapped in the dipole potential wells produced by the intracavity field. The spatial self-organization of molecules in the cavity is evident with decrease of the spreading parameter. In this simulation, 120 of the 200 molecules are trapped and rapidly cooled to 850 μK in around 0.2 ms. The remaining molecules are accelerated and eventually escape from the cavity. The latter happens because these molecules

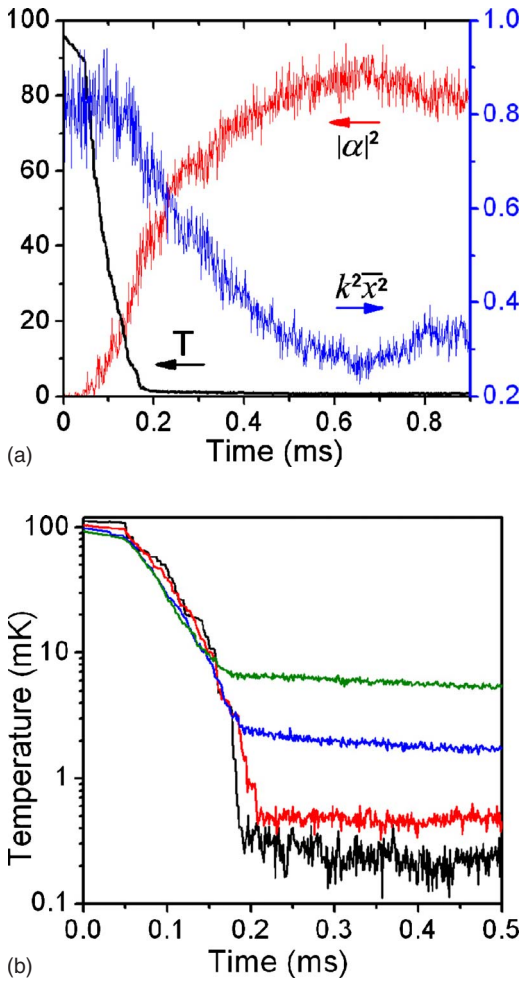

FIG. 2. (Color online) (a) Time evolution of the photon number $|\alpha|^2$ in the cavity (divided by 10 to fit the figure), the temperature of molecules (in mK), and the molecular spreading parameter $k^2\overline{x^2}$. (b) Temperature of the CN gas vs time for different initial molecular numbers in the cavity (from bottom to top, $N=50, 100, 400, 1000$).

are out of phase with the majority and do not benefit from the cavity-induced cooling process. We note that the pump intensity is high because a limited number of molecules are simulated for computational efficiency. According to the $1/N$ law discussed later in this paper, the pump intensity is reduced to about 1 kW/cm^2 to observe similar dynamics for 10^4 molecules. We have carried out many simulation runs with different initial temperatures and molecular numbers and show that, using the same pump intensity, molecules with initial temperature of 300 mK can be cooled to a similar final temperature on the same time scale. In general, for a given pump intensity, the number of trapped molecules is reduced on increasing their initial temperatures, while an increase of the pump intensity traps and cools more molecules. The number of trapped molecules also increases with increase of the cavity length. We have further found that, once the pump intensity is set above its threshold for cooling, the cooling time for the trapped molecules remains essentially unchanged for different molecular numbers and initial temperatures. Figure 2(b) shows the cooling process in time for different initial numbers of molecules with the same starting

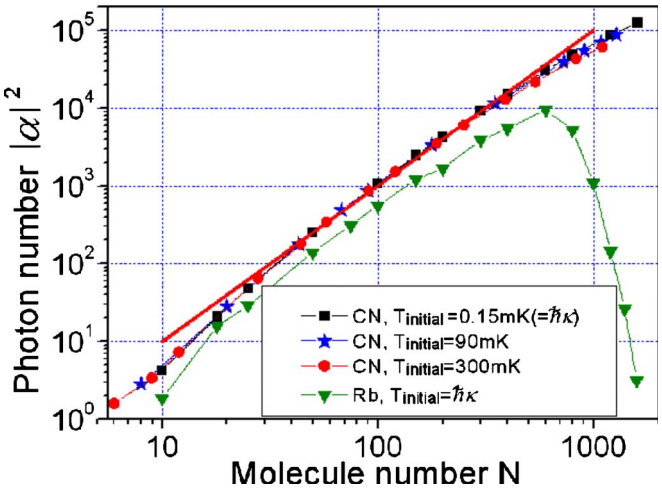

FIG. 3. (Color online) Relationship between photon number and molecular number for different initial temperatures for the CN molecular gas. The results for Rb atoms are also shown for comparison.

temperature. The jumps shown in the curves, which are more prominent in the cases of smaller molecular numbers, imply the loss of hot molecules from the cavity and consequently the reduction of temperature for molecules remaining in the cavity. The cooling time is around 0.2 ms for all cases. The final molecular temperature depends on the operating conditions of the system; a lower temperature is obtained when the system operates just above the pump threshold.

The averaged photon number in the cavity can be well approximated by the steady-state solution of Eq. (1) without the noise terms, which in the limit of large molecular detuning $\Delta_{aR1}, \Delta_{aQ21} \gg \gamma$, small molecular spreading $k^2x^2 \ll 1$, and the cavity detuning condition $\Delta_c = -\kappa + N_{tr}U_0$, is given as

$$\overline{|\alpha|^2} = N_{tr}^2 \frac{|\eta_{eff}|^2}{\kappa^2} \frac{(1 - k^2\overline{x^2})}{1 + [1 - (U_0 N_{tr}/\kappa)k^2x^2]^2}. \tag{5}$$

Here the number of trapped molecules N_{tr} in the cavity has replaced the initial molecular number N. This modification allows us to describe cases with different initial temperatures. As depicted in Fig. 3, the curves for initial temperatures of 0.15 (=$\hbar\kappa$), 90, and 300 mK are very close together and all obey the quadratic relation $\overline{|\alpha|^2} \propto N_{tr}^2$ in the parameter window around $N_{tr}=100$, where $k^2\overline{x^2}$ is small and the motions of the trapped molecules are well correlated. We also plot the curve for Rb atoms for comparison. Rb atoms behave in a similar way to CN molecules for $N_{tr} < 600$, beyond which, however, the photon number is rapidly reduced on increasing N_{tr}. The latter effect is due to the appearance of a significant number of stable defect molecules [11]. The stable defect molecules are those trapped in different types of wells from the majority, and they destroy the intracavity field through destructive interference with the rest. A simple theoretical estimation of the threshold for the occurrence of the defects is given as $N_{thr} = \kappa/|U_0| \approx 40$ for Rb atoms. Our simulations show that a noticeable number of defects appears at much higher molecular number, around $N=200$, and their percentage increases on further increasing the molecular number in the cavity; at $N=600$ the defects reach more than 5% and start to reduce the intracavity field. CN molecules have a much larger threshold, at $N_{thr} \approx 1200$, according to the estimation. Based on the results of Rb atoms, the same effect for CN molecules due to stable defects should appear at around $N=10^4$, which is beyond our simulation range. This finding shows that cavity cooling occurs only for a molecular gas whose number does not significantly exceed the threshold N_{thr} for the emergence of stable defects. This restriction will be further discussed later in this paper.

The observation that the quadratic relation $\overline{|\alpha|^2} \propto N_{tr}^2$ holds only in a limited parameter window is due to the fact that collective dynamics of molecules occurs only in a certain parameter region of the system. This is evident on examining the relation of molecular spreading $k^2\overline{x^2}$ with other parameters of the system. For example, while an increase of the molecular number deepens the potential trap, which compresses the molecular spatial size around the antinodes, it also increases the noise effects due to the increased intracavity field intensity, which tends to spread the molecular clouds and also raises the final molecular temperatures. To investigate its functional dependence on the parameters, we consider the dipole potential energy produced by the intracavity field intensity. When a molecule is cooled in the cavity, the averaged potential energy experienced by the molecule is, from the right-hand side of Eq. (1b),

$$\bar{U} = -\hbar \left[U_0 \left(\overline{|\alpha|^2} - \frac{1}{2} \right) \cos^2(\overline{kx}) + 2[\mathrm{Im}(\eta_{eff})\overline{\alpha_1} - \mathrm{Re}(\eta_{eff})\overline{\alpha_2}]\cos(\overline{kx}) \right] \tag{6}$$

where α_1 and α_2 are the real and imaginary parts of α. The averaged potential energy variation due to molecular spatial spreading from the antinodes of the field is therefore

$$|\Delta\bar{U}| = \hbar\{|U_0|\overline{|\alpha|^2}[1 - \cos^2(\overline{kx})] + 2|[\mathrm{Im}(\eta_{eff})\bar{\alpha}_1 - \mathrm{Re}(\eta_{eff})\overline{\alpha_2}]|[1 - |\cos(\overline{kx})|]\} \tag{7}$$

Here we have assumed $\overline{|\alpha|^2} \gg 1$. In the case of $\Delta_{aR1}, \Delta_{aQ21} \gg \gamma$, $|\overline{\alpha_1}| \approx |\overline{\alpha_2}| \approx |\alpha|/\sqrt{2}$, and $|\mathrm{Re}(\eta_{eff})| \ll |\mathrm{Im}(\eta_{eff})| \approx |\eta_{eff}|$. Equation (7) can be simplified in the limit of $k^2\overline{x^2} \ll 1$ to

$$|\Delta\bar{U}| \approx \hbar \left(|U_0||\alpha|^2 + |\eta_{eff}|\frac{|\alpha|}{\sqrt{2}} \right) k^2\overline{x^2}. \tag{8}$$

When the molecules reach the steady state, the potential energy difference given by Eq. (8) equals the kinetic energy. Since all degrees of freedom have the same energy $k_BT/2$, the relation $|\Delta\bar{U}| = k_BT/2$ gives

$$k^2\overline{x^2} \approx \frac{k_BT}{2\hbar} \left(|U_0||\alpha|^2 + |\eta_{eff}|\frac{|\alpha|}{\sqrt{2}} \right)^{-1}. \tag{9}$$

By substituting Eq. (5) into Eq. (9), we obtain the relation of the molecular spatial spreading with the number,

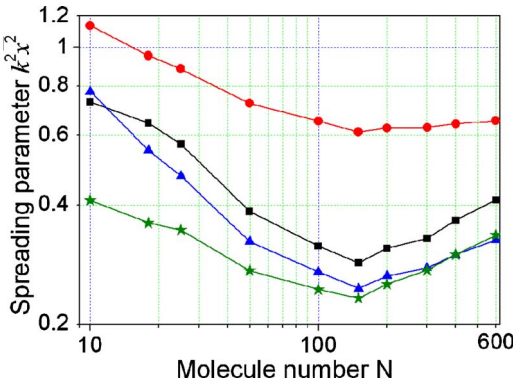

FIG. 4. (Color online) Spreading parameter vs molecular number. The square curve (black online) is generated directly from numerical integration of Eq. (1). The curve with triangles (blue online) is plotted using Eq. (9) with photon numbers and temperatures from numerical simulation. The curve with asterisks (olive online) is from Eq. (10). The curve with circles (red online) is produced using the expression from Ref. [11] for CN parameters for the purpose of comparison.

$$k^2\overline{x^2} \approx \frac{k_B T}{\hbar\kappa}\left(\frac{|\eta_{eff}|^2}{\kappa^2}N_{tr}\right)^{-1}, \tag{10}$$

where we have imposed the restriction $(|U_0|/\kappa)N_{tr} \ll 1$. For comparison, we have plotted three curves in the $(k^2\overline{x^2}, N)$ space in Fig. 4, which are obtained by using Eqs. (9) and (10) and directly from numerical results of Eq. (1). The curve generated by Eq. (9) fits well with the numerical results for different molecular numbers except in the small window just above the threshold, where collective dynamics has not been fully established and noise effects are relatively strong. The deviation of Eq. (10) from the numerical results is also mainly in the region of small N. This is because of the existence of a finite number of defect molecules in this region, and consequently Eq. (5) should be corrected by removing these molecules from N_{tr}. We note that Eq. (10) does not imply a simple $1/N_{tr}$ law, because the temperature also varies with the molecular numbers and its expression is not yet available. Our extensive numerical simulations show that the temperature increases monotonically with the molecular number once collective dynamics occurs ($N > 10$ in Fig. 4) and can be approximated by $T \propto a_0 + a_1 N_{tr} + a_2 N_{tr}^2$, where $a_0 \gg a_1 \gg a_2$. By substituting this relation into Eq. (10), we obtain $k^2\overline{x^2} \propto a_1 + a_0/N_{tr}$ for the region of small molecular numbers and $k^2\overline{x^2} \propto a_1 + a_2 N_{tr}$ for large molecular numbers. These functional dependences fit qualitatively with the curves in the figure. The above analysis and simulation show that, in cavity cooling, the pump intensity should be set in the region close to the threshold, in which the collective dynamics of molecules is strong and the final molecular temperature is low. We note that a different expression from Eq. (9) was obtained in Ref. [11] using a harmonic oscillation model and the $1/N$ law was suggested for a small window of molecular numbers where the changes of cooling temperature with molecular number are neglected. For comparison we have plotted this expression [Eq. (31) of Ref. [11]] using our simulation results of CN molecules. The curve captures the main features for a small number of molecules but is shifted significantly upward.

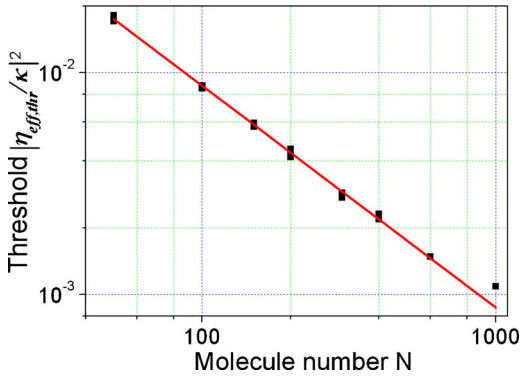

FIG. 5. (Color online) Numerical simulations show the $1/N$ law for the pump intensity threshold for CN molecules.

We have further investigated the relation of the pump intensity threshold to the molecular numbers. This relation is obtained based on our extensive numerical results on CN molecules. We start with a finite number of molecules N in uniform distribution in space and low initial temperature $(=\hbar\kappa)$. On increasing the pump intensity, the molecules tend to accumulate in either odd or even numbered potential wells through self-organization processing. The pump threshold is defined at the point where the statistical difference δN of the molecules around the odd and even wells equals the square root of the molecular number, i.e., $\delta N = \sqrt{N}$. Since the intracavity field fluctuates significantly in the region of the threshold, the pump intensity is determined using extensive numerical runs and statistical analysis. Figure 5 shows that the effective pump threshold is inversely proportional to the molecular number, i.e., $|\eta_{eff,thr}|^2 \propto 1/N$. Using Eq. (3) we have

$$|\eta_{thr}|^2 \propto \frac{(\Delta_{aR1}\Delta_{aQ21})^2}{(g_{R1}\Delta_{Q21} + g_{Q21}\Delta_{R1})^2}\frac{\kappa^2}{N}, \tag{11}$$

where we have assumed $\Delta_{aR1}, \Delta_{aQ21} \gg \gamma$. Equation (11) can be further simplified in the case that the pump frequency detuning is much larger than the frequency difference between the two transition lines, i.e., $\Delta_{aR1} \approx \Delta_{aQ21} \equiv \Delta_a$. We have from Eq. (11) under this condition

$$|\eta_{thr}|^2 \propto \frac{\Delta_a^2\kappa^2}{g^2 N}. \tag{12}$$

This relation implies that a smaller value of the coupling strength g for a certain molecular gas can be compensated by a larger molecular number in the cavity to have the same pump intensity threshold for cooling. For example, the transition strength of the relevant lines in CN molecules is some two orders of magnitude smaller than that in Rb atoms, and consequently a relatively small cavity mode volume was used in our CN simulations to boost the coupling strength. In fact, given by the relation (12), we can reduce the coupling strength and increase the molecular number at the same time to achieve effective cooling. We have verified this in simu-

lations. This relation therefore gives flexibility in cavity configurations for cooling molecules. We note that two different scaling laws have been suggested based on mean-field continuous and statistical models in the study of atoms in a cavity field [11], and they gave, respectively, $1/N$ and $1/\sqrt{N}$ laws with respect to the threshold for the pump intensity. While our definition for the pump intensity threshold follows the statistical model, and numerical simulations involve a limited number of molecules, we observe the $1/N$ law, as given by Eq. (12), which is consistent with the mean-field continuous analysis. We further note that there is a noticeable constant shift between the threshold values given in Fig. 5 and those derived from the mean-field analysis.

Finally, we discuss how the scaling relations given by Eqs. (5), (10), and (12) can be used to extend our results obtained based on the simulations of hundreds of molecules to a very large molecular ensemble. First, these relations are valid only when the number of molecules to be cooled in the cavity does not significantly exceed the threshold value N_{thr} for the appearance of stable defects. Since $N_{thr}=\kappa/|U_0|$, the dispersion parameter $|U_0|$ must be reduced and/or the cavity relaxation rate κ increased to increase N_{thr}. For example, for the value of κ given earlier, if the pump frequency detuning Δ_a ($|U_0|$) is increased (decreased) by five orders of magnitude, a gas of 10^9 CN molecules can be cooled in the cavity without the occurrence of significant stable defects. Thus, in order to cool an ensemble of 10^9 CN molecules, the pump field must be detuned further from the molecular resonance from the near-resonant regime (gigahertz to tens of gigahertz detuning) to far off resonance (detuning on the order of half the resonant transition frequency). The pump intensity threshold for molecular self-organization and cooling, as given by Eq. (12), is increased by four orders to 6×10^6 W/cm^2. This estimate shows that cavity cooling of a large molecular sample is possible by use of a far-off-resonant, high-intensity pump. In this new parameter set for cooling of a 10^9 CN molecular gas, the scaling relations of Eq. (5) and (10) should still be observed when molecules are self-organized above the pump threshold. The intracavity photon number in this case is increased by six orders of magnitude because of the scaling $\overline{|\alpha|^2}\propto N_{tr}^2|\eta_{eff}|^2$ given by Eq. (5), whereas the spatial spreading parameter remains unchanged due to the fact that $\overline{x_{nm}^{\ 2}}\propto(|\eta_{eff}|^2N_{tr})^{-1}$ given by Eq. (10). We note that varying κ gives more flexibility in the choice of the pump intensity and other parameters.

In summary, we have studied a cavity scheme for molecules and predicted, using an example, that CN molecules can be cooled from the 100 mK range to submillikelvin temperatures in less than 1 ms. While CN molecules have a complex energy level structure, the near-resonant interaction model can be simplified to comprise only three levels. This approach can be extended to other molecular species of current interest in cold molecule research for which the scaling laws discussed in this paper can be generalized. These results may therefore benefit researchers working on other species such as NH [14] and OH [15]. We note that the one-dimensional cavity model is a good approximation which captures the main results of a more complete description that includes the transverse effects [11]. Moreover, through the analysis of the scaling laws, it has shown that cavity cooling of a very large molecular sample is possible by use of a far-off-resonant, high-intensity pump. Interestingly, since far-off-resonant interactions do not rely on specific internal energy levels of particles, cavity cooling can in principle be realized for any polarizable species. We note that the molecule-field coupling in far off resonance is described by the polarizability of molecules which accounts for all transition lines. Further investigation is required to extend the current model to the far-off-resonance regime.

We would like to thank Dr. Peter Domokos, Professor Helmut Ritsch, and Dr. Guangjiong Dong for useful discussions.

[1] S. Chu, L. Hollberg, J. E. Bjorkholm, A. Cable, and A. Ashkin, Phys. Rev. Lett. **55**, 48 (1985).
[2] J. D. Weinstein, R. deCarvalho, T. Guillet, B. Friedrich, and J. M. Doyle, Nature (London) **395**, 148 (1998).
[3] J. M. Doyle, B. Friedrich, Jinha Kim, and David Patterson, Phys. Rev. A **52**, R2515 (1995).
[4] H. L. Bethlem, G. Berden, F. M. H. Crompvoets, R. T. Jongma, A. J. A. van Roij, and G. Meijer, Nature (London) **406**, 491 (2000).
[5] M. R. Tarbutt, H. L. Bethlem, J. J. Hudson, V. L. Ryabov, V. A. Ryzhov, B. E. Sauer, G. Meijer, and E. A. Hinds, Phys. Rev. Lett. **92**, 173002 (2004).
[6] P. Horak, G. Hechenblaikner, K. M. Gheri, H. Stecher, and H. Ritsch, Phys. Rev. Lett. **79**, 4974 (1997).
[7] P. Maunz, T. Puppe, I. Schuster, N. Syassen, P. W. H. Pinkse, and G. Rempe, Nature (London) **428**, 50 (2004).
[8] P. Domokos and H. Ritsch, J. Opt. Soc. Am. B **20**, 1098 (2003).
[9] P. Domokos and H. Ritsch, Phys. Rev. Lett. **89**, 253003 (2002).
[10] H. W. Chan, A. T. Black, and V. Vuletic, Phys. Rev. Lett. **90**, 063003 (2003).
[11] J. K. Asboth, P. Domokos, H. Ritsch, and A. Vukics, Phys. Rev. A **72**, 053417 (2005).
[12] R. Fulton, A. I. Bishop, M. N. Shneider, and P. F. Barker, Nat. Phys. **2**, 465 (2006).
[13] www.sri.com/psd/lifbase/
[14] D. Egorov, W. C. Campbell, B. Friedrich, S. E. Maxwell, E. Tsikata, L. D. van Buuren, and J. M. Doyle, Eur. Phys. J. D **31**, 307 (2004).
[15] S. Y. T. van de Meerakker, P. H. M. Smeets, N. Vanhaecke, R. T. Jongma, and G. Meijer, Phys. Rev. Lett. **94**, 023004 (2005).